DMM Advance Online Articles. Posted 24 August 2016 as doi: 10.1242/dmm.025288
Access the most recent version at http://dmm.biologists.org/lookup/doi/10.1242/dmm.025288

INSULIN RECEPTOR ISOFORM A AMELIORATES LONG TERM GLUCOSE INTOLERANCE IN DIABETIC MICE

Sabela Diaz-Castroverde[1,2,3], Almudena Gómez-Hernández[1,2], Silvia Fernández[1,2], Gema García-Gómez[1,2], Marianna Di Scala[4], Gloria González-Aseguinolaza[4], Elisa Fernández-Millán[1,2,3], Águeda González-Rodríguez[5], María García-Bravo[6], Pierre Chambon[7], Carmen Álvarez[1,2,3], Liliana Perdomo[1], Nuria Beneit[1], Oscar Escribano[1,2,3,8] and Manuel Benito[1,2,3,8].

[1]Department of Biochemistry and Molecular Biology II, School of Pharmacy, Complutense University of Madrid. 28040, Spain. [2]CIBER of Diabetes and Related Diseases (CIBERDEM), Health Institute Carlos III (ISCIII), Madrid, Spain. [3]Mechanisms of Insulin Resistance Consortium (MOIR), Madrid, Spain. [4]Division of Hepatology and Gene Therapy, Center for Applied Medical Research, University of Navarra, Pamplona, Navarra, 31008, Spain. [5]Liver Research Unit, Hospital Universitario Santa Cristina, Instituto de Investigación Sanitaria Princesa, Amadeo Vives 2, 28009 Madrid, Spain. Centro de Investigación Biomédica en Red de Enfermedades Hepáticas y Digestivas (CIBERehd), Barcelona, Spain. [6]Differentiation and Cytometry Unit, Hematopoietic Innovative Therapies Division, CIEMAT – CIBER of Rare Diseases (CIBERER) – Institute of Health Investigation Jiménez Díaz Foundation (IIS-FJD), Madrid, 28040, Spain [7]Institute of Genetic and Molecular and Cellular Biology (CNRS UMR7104; INSERM U596; ULP, Collége de France) and Mouse Clinical Institute. Illkirch, Strasbourg, 67400, France. [8] Co-senior authors

Correspondence should be addressed to O.E. (oescriba@ucm.es)

Keywords: glucose homeostasis, insulin receptor isoforms, adenoassociated virus (AAVs), liver.

SUMMARY STATEMENT

The specific hepatic expression of insulin receptor isoform A, but not B, is able to revert, in the long term, the global glucose intolerance observed in diabetic mice.

ABSTRACT

Type 2 diabetes mellitus is a complex metabolic disease and its pathogenesis involves abnormalities in both peripheral insulin action and insulin secretion. Previous *in vitro* data showed that insulin receptor isoform A, but not B, favours basal glucose uptake through its specific association with endogenous GLUT1/2 in murine hepatocytes and beta cells. With this background, we hypothesized that hepatic expression of insulin receptor isoform A in a mouse model of type 2 diabetes could potentially increase the glucose uptake of these cells decreasing the hyperglycaemia and therefore ameliorating the diabetic phenotype. To assure this hypothesis, we have developed recombinant adeno-associated viral vectors expressing insulin receptor isoform A or B under the control of a hepatocyte specific promoter. Our results demonstrate that in the long term, hepatic expression of insulin receptor isoform A in diabetic mice is more efficient than IRB ameliorating glucose intolerance. Consequently, it impairs the induction of compensatory mechanisms through beta-cell hyperplasia/hypertrophy that finally lead to beta-cell failure, reverting the diabetic phenotype in about 8 weeks. Our data suggest that long-term hepatic expression of insulin receptor isoform A could be a promising therapeutic approach for the treatment of type 2 diabetes mellitus.

Disease Models & Mechanisms • DMM • Advance article

INTRODUCTION

Type 2 diabetes mellitus (T2DM) results from a combination of insulin resistance and impaired insulin secretion, where insulin resistance has been described as the most important pathophysiological feature in prediabetic states (Kahn 1994, 1995). Insulin resistance affects several tissues that are relevant in glucose homeostasis such as liver, skeletal muscle and the adipose organ (Muoio and Newgard, 2008). In particular, hepatic insulin resistance is manifested by the blunted ability of insulin to activate its receptor kinase and its downstream targets, resulting in incomplete suppression of hepatic glucose production and therefore a manifest hyperglycaemia. As a compensatory mechanism, beta-cell hyperplasia/hypertrophy takes place to increase the insulin secretion that leads to hyperinsulinemia (Muoio and Newgard, 2008). Due to the central role of the liver in the control of glucose homeostasis, hepatic insulin resistance becomes a hallmark of T2DM (Michael et al., 2000; Cook et al., 2015), and, therefore, precise regulation of glucose homeostasis is a major challenge in diabetes management (Callejas et al., 2003).

The insulin receptor (IR) is a member of subclass II of the tyrosine kinase receptor super-family that plays an essential role in glucose metabolism (Benyoucef et al., 2007; Ward et al., 2009). IR is closely related to other members of this family like the insulin-like growth factor receptor (IGF-IR) which are involved in normal growth and development (Ward et al., 2009). In mammals, alternative splicing gives rise to two isoforms of IR: IRA and IRB. The isoform B has 12 additional amino acids encoded by the exon 11 (Whittaker et al., 2009). This sequence is located immediately downstream of the ligand binding domain but does not affect insulin binding affinity which is very similar between IRA and IRB (Whittaker et al., 2009; Menting et al., 2013). However, IRA has approximately 10 fold higher affinity for IGF-I and IGF-II than IRB (Malaguarnera and Belfiore, 2009). Moreover, IRA is predominantly expressed during foetal development and embryogenesis where enhances IGF-II effects (Frasca et al., 1999). In addition to its role in development, it has also been described that an increased IRA/IRB ratio can be observed in beta cells under certain pathophysiological conditions like insulin resistance. Therefore, these data suggest that the upregulation of IRA expression is not only involved in malignancies but also can be a compensatory mechanism by which beta-cell mass can be expanded in response to a higher insulin demand (Escribano et al., 2009). Conversely, IRB is predominantly expressed in adult tissues, including liver, where it triggers the metabolic effects of insulin (Malaguarnera and Belfiore, 2009). Although insulin does not stimulate glucose uptake in the liver, *in vitro* studies in neonatal hepatocytes and pancreatic beta cells demonstrate that IRA plays a direct role favouring glucose uptake promoting its specific association with endogenous glucose transporters (GLUT1 and

GLUT2) (Nevado et al., 2006; Escribano et al., 2015). Therefore, differences in the capability of glucose uptake can be associated with the presence/absence of IR isoforms or with changes in the ratio between them. Currently, the specific role of each IR isoform in T2DM is not completely understood.

To elucidate the role of IR isoforms, we took advantage of the capacity of recombinant adeno-associated vectors serotype 8 (AAV8) to deliver long-term expressed recombinant genes to the liver. These vectors have demonstrated an outstanding therapeutic potential in animal models for hepatic disorders of carbohydrate metabolism; for instance, correction of abnormal glycogen storage has been achieved (Alexander et al., 2008).

In the present study, we have used iLIRKO (inducible Liver Insulin Receptor KnockOut) mice, as a model of severe hepatic insulin resistance and T2DM. iLIRKO presents impaired glucose tolerance and fasted hyperinsulinemia without showing any hepatic dysfunction, a crucial difference with the previous reported LIRKO mice (Michael et al., 2000). We have generated AAV8 vectors expressing IRA or IRB under the control of a hepatocyte-specific promoter, alpha-1 antitrypsin promoter (Kramer et al., 2003) in order to study the hepatic function of each insulin receptor isoform on the diabetic phenotype of iLIRKO mice. In this manuscript, we report that only specific hepatic IRA expression by AAV8 in iLIRKO mice is able to decrease the hyperglycaemia and plasma insulin levels reverting the diabetic phenotype of these animals.

RESULTS

Generation and analysis of inducible Liver Insulin Receptor KnockOut (iLIRKO) mice.

iLIRKO mice were created by breeding mice carrying insulin receptor alleles modified with loxP sites flanking exon 4 (Brüning et al., 1998) with mice in which the tamoxifen-dependent Cre-ER^{T2} recombinase gene was located under the albumin promoter (Schuler et al., 2004). After weaning, animals were fed with soy-free diet for two weeks in order to decrease phytoestrogen levels that could compete for binding to the Cre-ER^{T2} recombinase. Afterwards, mice were fed for two weeks with tamoxifen diet to induce Cre translocation to the nucleus and the deletion of *Insr* exon 4. Even though glucose intolerance is associated with long-term administration of tamoxifen, for example in the treatment of breast cancer patients (Lipscombe et al., 2012), the fact that the animals were fed only 2 weeks with tamoxifen and Control mice do not show this effect support that the glucose intolerance is not due to the diet in any case. Thereafter, animals were fed with standard chow until sacrifice (Fig. 1A). Deletion of *Insr* exon 4 was analyzed by qPCR of genomic DNA samples isolated from the total pool of the liver from Control or iLIRKO mice, showing that IR was sufficiently reduced in iLIRKO mice as compared to controls (Fig. 1B).The *Insr* exon 4 deletion was also tested by RT-PCR in mRNA purified from the liver of Control or iLIRKO mice (Fig. 1C), revealing the functionality of the exogenous inducible recombinase. Western blotting confirmed targeted specific disruption of IR in the liver of iLIRKO mice. No effect has been observed in other tissues such as muscle and kidney (Fig. 1D). Histological analysis at 5 months of age revealed normal hepatic architecture with no evidence of hyperproliferative nodules or steatosis in iLIRKO mice. (Fig. 1E). There were no liver weight changes in iLIRKO mice as compared with Control mice (data not shown).

Insulin receptor deficiency in the liver causes marked glucose and insulin intolerance.

Glucose and insulin tolerance were significantly impaired in 3-month-old iLIRKO mice, and both effects were fully maintained along the time (Figs 2A,B). These mice developed a marked hyperinsulinemia, due to the compensatory insulin secretion from pancreatic beta cells (Fig. 2C). We next characterized beta-cell mass in Control and iLIRKO mice. According to the hyperinsulinemia, insulin staining revealed a significant increase in beta-cell mass by approximately two fold in iLIRKO *vs* Control mice at 9 months of age (Fig. 2D). Consistent with previous works, these results indicate that hepatic IR signaling is required for normal glucose homeostasis.

AAV-mediated IRA/B expression in the liver

To explore the importance of each IR isoform in the liver on the normalization of global glucose homeostasis, we generated recombinant adeno-associated virus serotype 8 vectors containing *INSR* A (AAV-IRA) or B (AAV-IRB) isoforms or the reporter genes, luciferase (luc) or green fluorescent protein (GFP) under the control of a liver specific promoter (Fig. 3A). Liver specificity was demonstrated by *in vivo* luciferase expression analysis comparing saline-injected *vs* AAV-luc-injected mice (Fig. 3B). To test the percentage of transduced hepatocytes, we injected $3x10^{10}$ vg/kg AAV-GFP in Control mice. The results show that about 95% of hepatocytes were GFP positive within two weeks after treatment, suggesting that this dose led to a robust hepatic transduction (Fig. 3C). Lower panels represent the negative control of GFP staining. We also analyzed GFP staining in pancreas from AAV-GFP-injected mice to assure the AAV8 virus hepatic tropism (Fig. 3D). As shown, no GFP staining was observed in the pancreas of these animals. These results rule out the possibility of IR isoforms expression within the pancreas owing to AAV8 incorporation in this tissue.

To assure whether the IR isoforms have a differential role in the reversion of the diabetic phenotype of iLIRKO mice we designed the experimental schedule shown in Fig. 4A. AAV vectors were administrated 20 weeks after birth, when iLIRKO mice achieved the diabetic phenotype and then we checked the evolution at different time points. Mice were sacrificed 28 weeks after treatment (Fig. 4A). Genomic levels of mouse *Insr* exon 4 were measured by qPCR in all the groups studied. The results showed similar mouse exon 4 deletion in liver homogenates from AAV-IRA-injected iLIRKO (iLIRKO IRA) and AAV-IRB-injected iLIRKO (iLIRKO IRB) compared to iLIRKO mice, indicating that all the IR expression observed after the AAV administration was coming from the AAV vectors carrying the human IR isoforms transgenes (Fig. 4B). After AAV administration, mice achieved the expression of the corresponding *INSR* isoform in the liver as analyzed by RT-PCR (Fig. 4C). Following determination of AAV-mediated IR expression in the liver, we examined protein levels by Western-blot. Twenty-eight weeks postvector injection, IRA or IRB expression was similar to that observed in Control mice, avoiding any side effects related to IR overexpression. There were no effects on protein expression in iLIRKO mice injected with AAV-luc (Fig. 4D). Even though IRA overexpression is associated with hepatocellular carcinoma, it is noteworthy to emphasize that there were no alterations in hepatic morphology/structure in either iLIRKO-IRA or iLIRKO-IRB mice even after 28 weeks of the AAV administration as assessed by Dr. Fernández-Aceñero, pathologist from San Carlos Clinic Hospital in Madrid (Spain). The quantitative pathology score obtained was similar in

the five groups studied revealing no liver alterations due to gene manipulation. Thus, our data indicate that long-term AAV-mediated expression of IRA or IRB meets the safety feature for a gene therapy approach. (Fig. 4E).

IRA expression in the liver improves glucose homeostasis

We next tested the effects of IRA or IRB hepatic expression on glucose homeostasis 2 and 4 months after vector injection. We performed glucose and insulin tolerance tests in iLIRKO mice just before vector injection and, 2 and 4 months after vector injection (Figs. 5A-C). Treatment with both vectors improved glucose and insulin tolerance. However, as shown in Figure 5B, it took 2 months upon injection of IRA, but not IRB, to restore blood glucose to the levels found in 5 month-old Control animals (Fig. 5A). Moreover, these differences between iLIRKO IRA or iLIRKO IRB remained 4 months after viral administration (Fig. 5C). These results suggest that IRA is more efficient in the long term than IRB restoring the global glucose homeostasis in iLIRKO mice. In this sense, we have evaluated several parameters regarding glucose and lipid metabolism. The most remarkable result is the significant increase in hepatic glycogen content observed in iLIRKO IRA mice compared to the other groups studied (Table S1). To investigate a potential underlying molecular mechanism involved, we performed immunoprecipitation assays searching the possible *in vivo* association between IR isoforms and GLUT2 (Fig. 5D). The results obtained show a significantly higher association between IRA and GLUT2 than those observed between IRB and GLUT2 in the corresponding iLIRKO mice. The histogram shows the quantification of band intensities (Fig. 5E).

IRA, but not IRB, expression in the liver induces a decreased beta-cell mass

Examination of beta-cell mass in iLIRKO IRA or iLIRKO IRB revealed that the improvement of hyperglycaemia induced by hepatic IRA expression has a direct effect on beta-cell plasticity. We found that plasma insulin levels were significantly decreased in iLIRKO IRA mice at 2 or 4 months upon injection as compared to the same mice (iLIRKO) before injection. By contrast, in iLIRKO IRB mice, plasma insulin levels remained elevated at 2 or 4 months upon AAV administration (Fig. 6A). As it is shown in a representative insulin staining (Figure 6B), quantification of fractional beta cell mass revealed an increase in iLIRKO mice compared to Control mice owing to the lack of insulin receptor. Regarding IR isoforms, our results

demonstrated a significant decrease in beta cell mass in iLIRKO IRA mice, but not in iLIRKO IRB mice, as compared to iLIRKO (Fig. 6C). According to this, iLIRKO mice showed an increase in the number of islets as compared to Control mice. However, we found a significant decrease in the number of islets in both, iLIRKO IRA or iLIRKO IRB mice, as compared with iLIRKO mice (Fig. 6D). The analysis of the islets size distribution revealed that the increased beta cell mass observed in iLIRKO IRB mice was due to a significant increase in the proportion of islets with medium size (1000-10000 μm^2) while the other groups studied showed a quite similar islet size distribution (Fig 6E). Taking together, these results provide clear evidence that expression of IRA or IRB in the liver is a crucial feature to control glucose homeostasis and, therefore, beta-cell mass.

To further characterize the mechanisms by which the beta-cell hyperplasia reverts in iLIRKO IRA mice we performed two different approaches. First, we stained pancreatic slides with insulin, DAPI and PCNA, a marker of cell proliferation when is located in nucleus (Fig. S1A). The counting of PCNA positive beta cells revealed significant differences between groups. There was a significant increase in iLIRKO mice compared to Control or iLIRKO IRA mice. However, we observed a complete absence of PCNA positive beta cells in iLIRKO IRB suggesting that the increase on beta-cell mass observed in this group could be related with hypertrophic beta cells (Fig. 7A). Secondly, we analyzed the pancreatic slides by TUNEL to determine the level of apoptosis in each condition (Fig. S1B). While the level of apoptosis was quite similar between Control, iLIRKO or iLIRKO IRA mice, we observed a significant decrease in iLIRKO IRB mice as compared with all group of mice studied (Fig. 7B). As a positive control, we analyzed pancreatic slides from neonatal rats since it has been shown a transient wave of apoptosis that occurs in developing rodent islets between the first and second week of postnatal life (Scaglia et al. 1997, Petrik et al. 1998). These results suggest that the hyperplasia observed in iLIRKO mice is reverted by a decrease in the beta-cell proliferation rather than an enhanced beta-cell apoptosis. As we have previously described, hepatic and circulating IGF-I levels are elevated in insulin-resistant iLIRKO mice, suggesting the presence of a liver-pancreatic endocrine axis (Escribano et al., 2009). Thus, we analyzed the hepatic expression of IGF-I in livers from Control, iLIRKO, iLIRKO IRA and iLIRKO IRB mice. Here, we show that the increase of IGF-I expression in the liver of iLIRKO mice is markedly downregulated by AAV-IRA treatment. However, in iLIRKO IRB, where glucose intolerance remains and the pancreatic beta-cell mass continues expanded (Fig. 7C), hepatic IGF-I levels remained elevated. These results suggest a correlation between hepatic IGF-I expression and glucose intolerance. Therefore, this data reinforce the fact that hepatic IRA in the long term, but not IRB, ameliorates glucose intolerance in iLIRKO mice (Figs.

5B,C). Moreover, regarding safety it is important to emphasize that the marked decrease of hepatic IGF-I expression in iLIRKO IRA mice lessens the possibility of an increased IGF-I/IRA signaling in the liver of these animals.

DISCUSSION

T2DM is a polygenic disease involving polymorphisms in genes encoding for proteins that participate in insulin signaling, insulin secretion and intermediary metabolism (Saltiel and Kahn, 2001). Animal models have provided major molecular insights into the role of different cellular pathways involved in the modulation of glucose homeostasis. How and to what extent these genes contribute to the human disease requires further investigation (Neubauer and Kulkarni, 2006).

The liver has the ability to rapidly adapt to blood glucose concentration changes due to its pivotal role in maintaining glucose homeostasis (El Ouaamari et al., 2016). However, its role in the progression from insulin resistance to fasting hyperglycemia has been ignored. Previous studies with conditional knockouts and reconstitution models concluded that, the progression of insulin resistance to diabetes with fasting hyperglycaemia requires defects in tissues other than liver. Moreover, constitutive deletion of IR in the liver has been reported to impair insulin signaling but does not induce chronic insulin resistance or hyperinsulinemia probably due to the hepatic dysfunction developed in these mice (Michael et al., 2000). However, our results in iLIRKO mice showed that the inducible liver-specific disruption of IR gives rise to chronic glucose intolerance and hyperinsulinemia without showing any hyperplasic nodules. This mouse model demonstrated that primary hepatic insulin resistance is necessary and sufficient to generate the progressive pathogenesis of T2DM (Escribano et al., 2009).

The unbalanced insulin signaling through compensatory hyperinsulinemia (Malaguarnera and Belfiore, 2011) also characterizes T2DM. It has been shown that in insulin resistant states, insulin loses its ability to suppress glucose production but it largely retains its capacity to drive lipogenesis (Cook et al., 2015). This selective insulin resistance in T2DM has important implications for therapy. It seems preferable to search for new agents that will improve insulin sensitivity in the pathway leading to suppression of hepatic gluconeogenesis as well as agents able to enhance glucose uptake in order to decrease the hyperglycaemia (Brown and Goldstein, 2008). In this sense, our group reported *in vitro* that presence/absence of one or another IR isoform

involves changes on the metabolic profile, concisely the expression of IRA, but not IRB, improves the glucose uptake in murine hepatocytes and beta cells by its association with GLUTs (Nevado et al., 2006; Escribano et al., 2015). More recent studies have shown a direct relationship between the metabolic status of T2DM patients and the IRA/IRB ratio suggesting a dynamic regulation of IR splicing depending on the metabolic profile (Besic et al., 2015). Since the affinity for insulin is almost identical in both isoforms (Whittaker et al., 2002; Menting et al., 2013) and glucose uptake is insulin-independent in the liver, these changes cannot be related to insulin binding. For all these reasons, it is necessary to dissect the role of each isoform *in vivo* in the liver in a context of T2DM.

In this study, we used iLIRKO mice as a model of T2DM. This model has shown that initial hepatic insulin resistance obtained by insulin receptor deficiency is compensated by a marked hyperinsulinemia, achieved by beta-cell hyperplasia. On this regard, we now provide convincing evidence showing that the increased beta-cell mass in response to hepatic insulin resistance previously described in iLIRKO mice (Escribano et al., 2009) was directly related to an increased number of beta-cell islets, without changes in their size. Our results demonstrate that global insulin resistance and therefore glucose homeostasis can be modified in the long term by expressing IRA, but not IRB, in the liver. Selective expression of IRA was able to restore glucose and insulin tolerance while IRB only partially improved insulin sensitivity. Moreover, association between GLUT2 and IRβ was significantly increased in iLIRKO IRA as compared to iLIRKO IRB. These results agreed to previous i*n vitro* studies that showed the same association in IRA-expressing hepatocytes, which was related with an increased glucose uptake (Nevado et al., 2006). Having in mind that hyperglycaemia is only importantly decreased in iLIRKO IRA, this could be one of the mechanism involved in the differential improvement of glucose intolerance. In fact, the favored association between GLUT2 and IRβ in iLIRKO IRA mice suggests that it is a matter of insulin receptor structure, due to the presence/absence of exon 11, instead of structural changes induced upon ligand binding, given the fact that both isoforms present the same affinity for insulin. Moreover, we have found that IRA expression *in vivo* favors insulin signaling on GSK3α/β phosphorylation inducing an increased glycogen synthesis (unpublished data), suggesting that IRA expression not only increase the glucose uptake by the hepatocytes, but also favor the downstream signaling leading to an increase in glycogen storage**.** In addition, we observed a maintained recovery of insulin levels in iLIRKO IRA mice that was accompanied by a decrease in beta-cell mass down to control values. These results suggest that, as occurs under physiological conditions such as pregnancy, where beta-cell mass decreases to normal values when insulin resistance remises after delivery, pancreatic beta-cell mass adapts to the

improvement of hepatic insulin sensitivity by regulating its size (Sorenson and Brelje, 1997; Scaglia et al., 1997; Huang et al., 2009; Rieck and Kaestner, 2010). In the case of IRB-injected mice, beta-cell mass and plasma insulin levels were similar to those observed in untreated iLIRKO. These results demonstrate that insulin resistance persists in iLIRKO IRB mice suggesting a differential role of both isoforms in the regulation of glucose homeostasis.

Because insulin resistance affects all tissues in the body, it is a challenge to identify the signals that promote islet growth in insulin-resistant states. Based on the absence of detectable increase of beta-cell mass in other than the liver tissue-specific models of insulin resistance (Bruning et al., 1998; Kulkarni et al., 1999; Bruning et al., 2000), it is tempting to speculate that the liver controls beta-cell mass in insulin resistant states. In fact, we previously described that different percentages of hepatic insulin receptor deletion correlated with the level of insulin resistance and also with the corresponding increase in beta-cell mass, suggesting that the level of hepatic insulin resistance causes a proportional increase in beta-cell mass (Escribano et al., 2009). The signals and proteins that mediate islet compensatory response to insulin resistance are currently poorly understood. In this sense, glucose has been reported to promote beta-cell growth (Bonner-Weir et al., 1989; Assmann et al., 2009) and is a putative candidate in the induction of beta-cell hyperplasia found in iLIRKO mice, which manifest a marked hyperglycaemia. Moreover, we have also described that in iLIRKO mice the expression of hepatic IGF-I is augmented and correlates with an increase on circulating IGF-I levels. In fact, IGF-I levels were correlated to the level of hepatic insulin resistance (Escribano et al., 2009). Thus, our results show that the increased hepatic expression of IGF-I observed in iLIRKO mice decreased in iLIRKO IRA, but not in iLIRKO IRB mice. The lowering of IGF-I lessens the possibility of an enhanced activation of the IRA/IGF-I axis that could be related to liver hyperplastic cells. In this sense, although IRA overexpression has been found in tumor samples of Hepatocellular Carcinoma, it seems that is not a causal factor but a consequence of the activation of other pathways such as EGFR (Chettouh et al., 2013). In any case, as we mentioned before, in this study we precluded IRA overexpression as a caution. In addition, hepatic IGF-I levels are well correlated with the hyperglycaemia, suggesting that both factors could be involved in beta-cell growth. Based on these results, it is tempting to speculate that elevated IGF-I plasma levels could become a biomarker of hepatic insulin resistance.

Finally, to further investigate the regression of beta-cell mass observed in iLIRKO IRA mice, beta-cell proliferation and apoptosis was measured. Adult beta cells proliferate at a very slow rate in basal physiological conditions (Teta et al., 2005; Dhawan et al., 2007; Meier et al., 2008; Pearl et al., 2010). However, in a pathological situation like the insulin resistance observed in iLIRKO

mice, the proliferation rate was increased. Our results show that hepatic IRA expression was able to reduce islet mass through decreasing beta-cell proliferation rate down to control values, without significant alterations in pancreatic beta cell apoptosis.

Altogether, this study highlights the central and complex role played by hepatic insulin receptor isoforms in the control of glucose metabolism. Based on these findings, *in vivo* long term AAV-mediated hepatic expression of IRA, but not IRB, could act as a glucose uptake promoter regulating hyperglycaemia, improving glucose homeostasis, precluding beta-cell mass expansion and therefore, avoiding the final beta-cell failure.

MATERIALS AND METHODS

Mice and diets

$IR^{(lox/lox)}$ mice were created by homologous recombination using an insulin receptor gene targeting vector with *lox*P sites flanking exon 4 (Bruning et al., 1998). For liver-specific deletion we used transgenic mice with the tamoxifen-dependent Cre-ER^{T2} recombinase coding sequence located under the control of the albumin promoter (Schuler et al., 2010). The iLIRKO mice were generated crossing C57Bl/6 $IR^{(lox/lox)}$ and heterozygous C57Bl/6 Alb-Cre-ER^{T2}, littermates $IR^{(lox/lox)}$ were used as control. Genotyping of the $IR^{(lox/lox)}$ and Alb-Cre-ER^{T2} transgenic mice was performed by PCR using genomic DNA isolated from the tip of the tail of 3- to 4-week-old mice as previously described (Schuler et al., 2010, Escribano et al., 2009). After weaning, iLIRKO and Control mice ($IR^{(lox/lox)}$) were fed with a soy free diet (RMS-0909-US-EN-02-DS-2016, Harlan Teklad, Barcelona, Spain) for two weeks followed by two weeks of tamoxifen diet (TD.09327, Harlan) in order to induce the Cre translocation to the nucleus (Schuler et al., 2010). After that, animals were fed with a standard chow *ad libitum*. Only male animals were studied and maintained on a 12-hour light-dark cycle. All animal experimentation was conducted in accordance with the accepted standards of animal use approved by the Complutense University of Madrid Committee.

Viral Constructs and Vector Production and Purification

Recombinant AAV vectors were constructed with a transgene cassette encoding sequence for the individual spliced isoforms of the *INSR* either containing or lacking exon 11 (IRB and IRA, respectively) single chain or the reporter *luc* under the regulation of a liver specific promoter, *α1-antitrypsin* (*AAT*). Coding sequences for the human IR isoforms were a generous gift of C.R. Kahn (Joslin Diabetes Center, Boston, MA). The transgene cassette was flanked by AAV2 wild type inverted terminal repeats. rAAV8 vectors were produced as previously described (Gil-Farina et al., 2013) Viral titers were determined by qPCR, performed three times in triplicate at three different dilutions.

AAV administration

5-month-old mice were injected intravenously with the AAVs. For all procedures, animals were anesthetized by intraperitoneal (IP) injection of a mixture of xylacine (Rompun 2%, Bayer, Leverkusen, Germany) and ketamin (Imalgene 50, Merial, Lyon, France) 1:9 v/v.

Immunoprecipitation and Western blot

Tissues were homogenized as described (Bruning et al., 1998). Western blot analyses of insulin signaling proteins were performed on liver homogenates as previously described (Valverde et al., 1998). For immunoprecipitation, after protein content determination, equal amounts of protein (400 µg) were immunoprecipitated overnight at 4ºC with GLUT-2 antibodies (C-19) from Santa Cruz Biotechnology (Dallas, TX, USA). The immune complexes were collected on protein A-agarose beads and submitted to SDS-PAGE. For Western blot, the antibodies used were anti-insulin receptor β subunit (sc-711), anti-GLUT-2 (H-67) and anti-IGF-I (sc-9013) from Santa Cruz Biotechnology (Dallas, TX) and anti-β-actin from Sigma-Aldrich (St. Louis, MO). Rabbit and mouse primary antibodies were immunodetected using horseradish peroxidase-conjugated polyclonal anti-rabbit or mouse antibodies respectively (GE Healthcare, Buckinghamshire, UK). Loading was normalized by β-actin. The band intensities were quantified using ImageJ software (http://rsb.info.nih.gov/ij).

Metabolic tests

Glucose tolerance tests (GTT) were performed by intraperitoneal administration 2g/kg body weight of glucose after a 16h overnight fast. Blood glucose was monitored using Accu-Check blood glucose strips and glucometer (Roche, Penzberg, Germany). Insulin tolerance tests (ITT) were performed in the random fed state at 11am. Animals were injected with 1U/kg body weight of human regular insulin (Humulin regular, Eli Lilly, Indianapolis, IN) and blood glucose levels were measured at indicated times. ITT data are presented as percentage of initial blood glucose concentration. Insulin ELISA (Millipore, Billerica, MA) was performed with plasma samples obtained from 16h overnight fasted mice. Total cholesterol kit (Wako, Saitama, Japan) and total triglycerides kit (Thermo Fisher, Waltham, MA) were used with plasma and liver samples obtained from 24h fasted followed of 1h refed mice. Hepatic lipids were isolated as described (Folch *et al.*, 1957).

mRNA and genomic DNA expression

Liver RNA was prepared using Trizol (Life Technologies, Carlsbad, CA), cDNA was synthesized using High Capacity reaction kit (Applied Biosystems, Carlsbad, CA) and PCR was performed with DNA AmpliGel Master Mix (Biotools, Madrid, Spain). Genomic DNA from liver was extracted with DNA purification system (Promega, Madison, WI) and qPCR was performed using FastStart Universal SYBR green master mix (Roche) using the forward primer (intron 3) 5'-GTCCGCTTGTCCCACCAG-3' and reverse primer (exon 4) 5'-CAATGGTCTTCTCACCTTCG-3'. The primers used to determine the deletion of the exon 4 were 5'-CTGTTCGGAACCTGATGAC-3´ and 5´-ATACCAGAGCATAGGAG-3´. Primers flanking the human exon 11 were 5´-AGGAAGACGTTTGAGGATT-3´ and 5´-CACCGTCACATTCCCAACAT-3´. A 316 bp band corresponds to IRB isoform and 280 bp to IRA isoform.

Immunohistochemistry, Immunofluorescence, Islet Morphometry and Analysis of Cell Proliferation

Tissues samples were fixed overnight in 4% formaldehyde in 10% neutral buffered and routinely paraffin-embedded. Each liver block was serially sectioned (7μm) and hematoxilin/eosin stained using standard techniques. For GFP staining, we used GFP antibodies (B-2, Santa Cruz Biotechnology, Dallas, TX) and the corresponding negative controls were performed in the same samples without GFP primary antibodies. Total GFP-positive and GFP-negative cell number per section was counted to evaluate the transduction percentage. At least, 1500 hepatocytes were counted per liver.

Each pancreatic or hepatic block was then serially sectioned (5μm) throughout its length to avoid any bias due to regional changes in islet distribution and islet cell composition and was mounted on slides. Sections at fixed intervals throughout the block (every 72nd section) were incubated with guinea pig antibodies against insulin (Abcam, Cambridge, UK) or Ki-67 (Dako, Glostrup, Denmark). Visualization of immunocomplexes was carried out using appropriate secondary antibodies and a diaminobenzidine substrate kit for peroxidase (Agilent Technologies, Santa Clara, CA). Beta-cell fractional area was determined by calculating the ratio between the area occupied by insulin-positive cells and that occupied by total pancreatic cells. The total islet number per section (square millimeters of pancreatic tissue) was counted, and islets were arbitrarily classified by their area (square micrometers) to evaluate the distribution of islet sizes.

Proliferating beta cells were identified for PCNA nucleus location by co-staining for PCNA (F-2, Santa Cruz Biotechnology, Dallas, TX), DAPI and insulin. Beta-cell replication rate was expressed as the percentage of PCNA-positive beta cells. At least, 1500 beta cells were counted per pancreas. Beta-cell apoptosis was estimated by TUNEL assay (ApopTag Peroxidase In Situ Apoptosis Detection Kit, Millipore) coupled to insulin staining as previously described (Miguel-Santos et al. 2010) and the beta-cell apoptosis rate was expressed as the percentage of apoptotic-positive beta cells. Images of stained sections were acquired using a digital camera (XCD-U100CR, Sony, Tokyo, Japan) attached to a light microscope (Eclipse 8i, Nikon, Tokyo, Japan). Morphometric analyses were performed with automated image analysis software (Histolab, Microvision Instruments, Gothenburg, Sweden).

Bioluminescence imaging

Mice were immobilized with intraperitoneal anesthesia (a mixture of xylacine and ketamine). The substrate luciferin (150 µg/kg dissolved in phosphate-buffered saline; Promega, Madison, WI) was intraperitoneally injected. Ten minutes later, animals were placed in the dark chamber for light acquisition in an IVIS charge-coupled device camera system (Xenogen, Alameda, CA) and analyzed with the Living Image 2.20 software package (Xenogen, Alameda, CA). A region of interest covering the whole animal was defined, and quantification of light emission was performed in photons/second. Time exposure ranged from 1 second to 5 minutes depending on light intensity.

Statistical Analysis

The data are presented as means ± SEM from at least three independent experiments. Regarding *in vivo* experiments we used at least four mice. Differences between two groups were assessed using unpaired two-tailed *t*-tests. Data involving more than two groups were assessed by analysis of variance (ANOVA). A p value of <0.01 was considered statistically significant.

ACKNOWLEDGEMENTS

The authors want to thank to C.R. Kahn for the gift of the human insulin receptor sequences and María Jesús Fernández-Aceñero for her helpful assistance with the pathohistological analysis.

COMPETING INTERESTS

No competing interests declared

AUTHOR CONTRIBUTIONS

SD-C has participated in the acquisition, analysis and interpretation of data, design the experiments and wrote the paper. MD and GG-A have designed the AAVs. AG-H, SF, GG-G, EF-M, MG-B, LP, CA, AG-R and NB have participated in the acquisition, analysis and interpretation of data. PC generated the Alb-Cre ERT^2 mice. OE has participated in the design and coordination of the study, analysis and interpretation of data and wrote the manuscript. MB has participated in the design and coordination of the study and wrote the manuscript. All authors discussed the results and approved the final manuscript.

FUNDING

This work was supported by grants SAF2011/22555 and SAF2014-51795-R from Ministerio de Ciencia e Innovación, Comunidad de Madrid (S2010/BMD-2423) and CIBER de Diabetes y Enfermedades Metabólicas Asociadas (CIBERDEM) project (PIE14/00061), Instituto de Salud Carlos III, Spain.

REFERENCES

Alexander, I. E., Cunningham, S. C., Logan, G. J. and Christodoulou, J. (2008). Potential of AAV vectors in the treatment of metabolic disease. *Gene Ther* **15**, 831-839.

Assmann, A., Ueki, K., Winnay, J. N., Kadowaki, T. and Kulkarni, R. N. (2009). Glucose effects on beta-cell growth and survival require activation of insulin receptors and insulin receptor substrate 2. *Mol Cell Biol* **29**, 3219-3228.

Benyoucef, S., Surinya, K. H., Hadaschik, D. and Siddle, K. (2007). Characterization of insulin/IGF hybrid receptors: contributions of the insulin receptor L2 and Fn1 domains and the alternatively spliced exon 11 sequence to ligand binding and receptor activation. *Biochem J* **403**, 603-613.

Besic, V., Shi, H., Stubbs, R. S. and Hayes, M. T. (2015). Aberrant liver insulin receptor isoform A expression normalises with remission of type 2 diabetes after gastric bypass surgery. *PLoS One*. **5**: e0119270.

Bonner-Weir, S., Deery, D., Leahy, J. L. and Weir, G. C. (1989). Compensatory growth of pancreatic beta-cells in adult rats after short-term glucose infusion. *Diabetes* **38**, 49-53.

Brown, M. S. and Goldstein, J. L. (2008). Selective versus total insulin resistance: a pathogenic paradox. *Cell Metab* **7**, 95-96.

Bruning, J. C., Gautam, D., Burks, D. J., Gillette, J., Schubert, M., Orban, P. C., Klein, R., Krone, W., Muller-Wieland, D. and Kahn, C. R. (2000). Role of brain insulin receptor in control of body weight and reproduction. *Science* **289**, 2122-2125.

Bruning, J. C., Michael, M. D., Winnay, J. N., Hayashi, T., Horsch, D., Accili, D., Goodyear, L. J. and Kahn, C. R. (1998). A muscle-specific insulin receptor knockout exhibits features of the metabolic syndrome of NIDDM without altering glucose tolerance. *Mol Cell* **2**, 559-569.

Callejas, D., Mann, C. J., Ayuso, E., Lage, R., Grifoll, I., Roca, C., Andaluz, A., Ruiz-de Gopegui, R., Montane, J., Munoz, S. et al. (2013). Treatment of diabetes and long-term survival after insulin and glucokinase gene therapy. *Diabetes* **62**, 1718-1729.

Chettouh, H., Fartoux, L., Aoudjehane, L., Wendum, D., Clapéron, A., Chrétien, Y., Rey, C., Scatton, O., Soubrane, O., Conti, F., et al. (2013). Mitogenic insulin receptor-A is overexpressed in human hepatocellular carcinoma due to EGFR-mediated dysregulation of RNA splicing factors. *Cancer Res*. **73**, 3974-86.

Cook, J. R., Langlet, F., Kido, Y. and Accili, D. (2015). Pathogenesis of selective insulin resistance in isolated hepatocytes. *J Biol Chem* **290**, 13972-13980.

Dhawan, S., Georgia, S. and Bhushan, A. (2007). Formation and regeneration of the endocrine pancreas. *Curr Opin Cell Biol* **19**, 634-645.

El Ouaamari, A., Kawamori, D., Dirice, E., Liew, C. W., Shadrach, J. L., Hu, J., Katsuta, H., Hollister-Lock, J., Qian, W. J., Wagers, A. J. et al. (2013). Liver-derived systemic factors drive beta cell hyperplasia in insulin-resistant states. *Cell Rep* **3**, 401-410.

Escribano, O., Gomez-Hernandez, A., Diaz-Castroverde, S., Nevado, C., Garcia, G., Otero, Y. F., Perdomo, L., Beneit, N. and Benito, M. (2015). Insulin receptor isoform A confers a higher proliferative capability to pancreatic beta cells enabling glucose availability and IGF-I signaling. *Mol Cell Endocrinol* **409**, 82-91.

Escribano, O., Guillen, C., Nevado, C., Gomez-Hernandez, A., Kahn, C. R. and Benito, M. (2009). Beta-Cell hyperplasia induced by hepatic insulin resistance: role of a liver-pancreas endocrine axis through insulin receptor A isoform. *Diabetes* **58**, 820-828.

Folch J, Lees M, Sloane Stanley GH (1957). A simple method for the isolation and purification of total lipides from animal tissues *J Biol Chem* **226**:497-509.

Frasca, F., Pandini, G., Scalia, P., Sciacca, L., Mineo, R., Costantino, A., Goldfine, I. D., Belfiore, A. and Vigneri, R. (1999). Insulin receptor isoform A, a newly recognized, high-affinity insulin-like growth factor II receptor in fetal and cancer cells. *Mol Cell Biol* **19**, 3278-3288.

Gil-Farina, I., Di Scala, M., Vanrell, L., Olague, C., Vales, A., High, K. A., Prieto, J., Mingozzi, F. and Gonzalez-Aseguinolaza, G. (2013). IL12-mediated liver inflammation reduces the formation of AAV transcriptionally active forms but has no effect over preexisting AAV transgene expression. *PLoS One* **8**, e67748.

Huang, C., Snider, F. and Cross, J. C. (2009). Prolactin receptor is required for normal glucose homeostasis and modulation of beta-cell mass during pregnancy. *Endocrinology* **150**, 1618-1626.

Kahn, C. R. (1994). Banting Lecture. Insulin action, diabetogenes, and the cause of type II diabetes. *Diabetes* **43**, 1066-1084.

Kahn, C. R. (1995). Diabetes. Causes of insulin resistance. *Nature* **373**, 384-385.

Kramer, M. G., Barajas, M., Razquin, N., Berraondo, P., Rodrigo, M., Wu, C., Qian, C., Fortes, P. and Prieto, J. (2003). In vitro and in vivo comparative study of chimeric liver-specific promoters. *Mol Ther* **7**, 375-385.

Kulkarni, R. N., Bruning, J. C., Winnay, J. N., Postic, C., Magnuson, M. A. and Kahn, C. R. (1999). Tissue-specific knockout of the insulin receptor in pancreatic beta cells creates an insulin secretory defect similar to that in type 2 diabetes. *Cell* **96**, 329-339.

Lipscombe, L. L., Fischer, H. D., Yun, L., Gruneir, A., Austin, P., Paszat, L., Anderson, G. M. and Rochon, P. A. (2012). Association between tamoxifen treatment and diabetes: a population-based study. *Cancer* **118**, 2615-2622.

Malaguarnera, R. and Belfiore, A. (2011). The insulin receptor: a new target for cancer therapy. *Front Endocrinol (Lausanne)* **2**, 93.

Meier, J. J., Butler, A. E., Saisho, Y., Monchamp, T., Galasso, R., Bhushan, A., Rizza, R. A. and Butler, P. C. (2008). Beta-cell replication is the primary mechanism subserving the postnatal expansion of beta-cell mass in humans. *Diabetes* **57**, 1584-1594.

Menting, J. G., Whittaker, J., Margetts, M. B., Whittaker, L. J., Kong, G. K., Smith, B. J., Watson, C. J., Zakova, L., Kletvikova, E., Jiracek, J. et al. (2013). How insulin engages its primary binding site on the insulin receptor. *Nature* **493**, 241-245.

Michael, M. D., Kulkarni, R. N., Postic, C., Previs, S. F., Shulman, G. I., Magnuson, M. A. and Kahn, C. R. (2000). Loss of insulin signaling in hepatocytes leads to severe insulin resistance and progressive hepatic dysfunction. *Mol Cell* **6**, 87-97.

Miguel-Santos L, Fernández-Millán E, Angeles Martín M, Escrivá F, Alvarez C. (2010). Maternal undernutrition increases pancreatic IGF-2 and partially suppresses the physiological wave of beta-cell apoptosis during the neonatal period. *J Mol Endocrinol* **44**, 25-36.

Muoio, D. M. and Newgard, C. B. (2008). Mechanisms of disease:Molecular and metabolic mechanisms of insulin resistance and beta-cell failure in type 2 diabetes. *Nat Rev Mol Cell Biol* **9**, 193-205.

Neubauer, N. and Kulkarni, R. N. (2006). Molecular approaches to study control of glucose homeostasis. *ILAR J* **47**, 199-211.

Nevado, C., Valverde, A. M. and Benito, M. (2006). Role of insulin receptor in the regulation of glucose uptake in neonatal hepatocytes. *Endocrinology* **147**, 3709-3718.

Perl, S., Kushner, J. A., Buchholz, B. A., Meeker, A. K., Stein, G. M., Hsieh, M., Kirby, M., Pechhold, S., Liu, E. H., Harlan, D. M. et al. (2010). Significant human beta-cell turnover is limited to the first three decades of life as determined by in vivo thymidine analog incorporation and radiocarbon dating. *J Clin Endocrinol Metab* **95**, E234-239.

Petrik, J., Arany, E., McDonald, T. J. and Hill, D. J. (1998) Apoptosis in the pancreatic islet cells of the neonatal rat is associated with a reduced expression of insulin-like growth factor II that may act as a survival factor. *Endocrinology*. **6,** 2994-3004.

Rieck, S. and Kaestner, K. H. (2010). Expansion of beta-cell mass in response to pregnancy. *Trends Endocrinol Metab* **21**, 151-158.

Saltiel, A. R. and Kahn, C. R. (2001). Insulin signalling and the regulation of glucose and lipid metabolism. *Nature* **414**, 799-806.

Scaglia, L., Cahill, C. J., Finegood, D. T. and Bonner-Weir, S. (1997). Apoptosis participates in the remodeling of the endocrine pancreas in the neonatal rat. *Endocrinology* **138**, 1736-1741.

Schuler, M., Dierich, A., Chambon, P. and Metzger, D. (2004). Efficient temporally controlled targeted somatic mutagenesis in hepatocytes of the mouse. *Genesis* **39**, 167-172.

Sorenson, R. L. and Brelje, T. C. (1997). Adaptation of islets of Langerhans to pregnancy: beta-cell growth, enhanced insulin secretion and the role of lactogenic hormones. *Horm Metab Res* **29**, 301-307.

Teta, M., Long, S. Y., Wartschow, L. M., Rankin, M. M. and Kushner, J. A. (2005). Very slow turnover of beta-cells in aged adult mice. *Diabetes* **54**, 2557-2567.

Valverde, A. M., Lorenzo, M., Pons, S., White, M. F. and Benito, M. (1998). Insulin receptor substrate (IRS) proteins IRS-1 and IRS-2 differential signaling in the insulin/insulin-like growth factor-I pathways in fetal brown adipocytes. *Mol Endocrinol* **12**, 688-697.

Ward, C. W. and Lawrence, M. C. (2009). Ligand-induced activation of the insulin receptor: a multi-step process involving structural changes in both the ligand and the receptor. *Bioessays* **31**, 422-434.

Whittaker, J., Sorensen, H., Gadsboll, V. L. and Hinrichsen, J. (2002). Comparison of the functional insulin binding epitopes of the A and B isoforms of the insulin receptor. *J Biol Chem* **277**, 47380-47384.

Figures

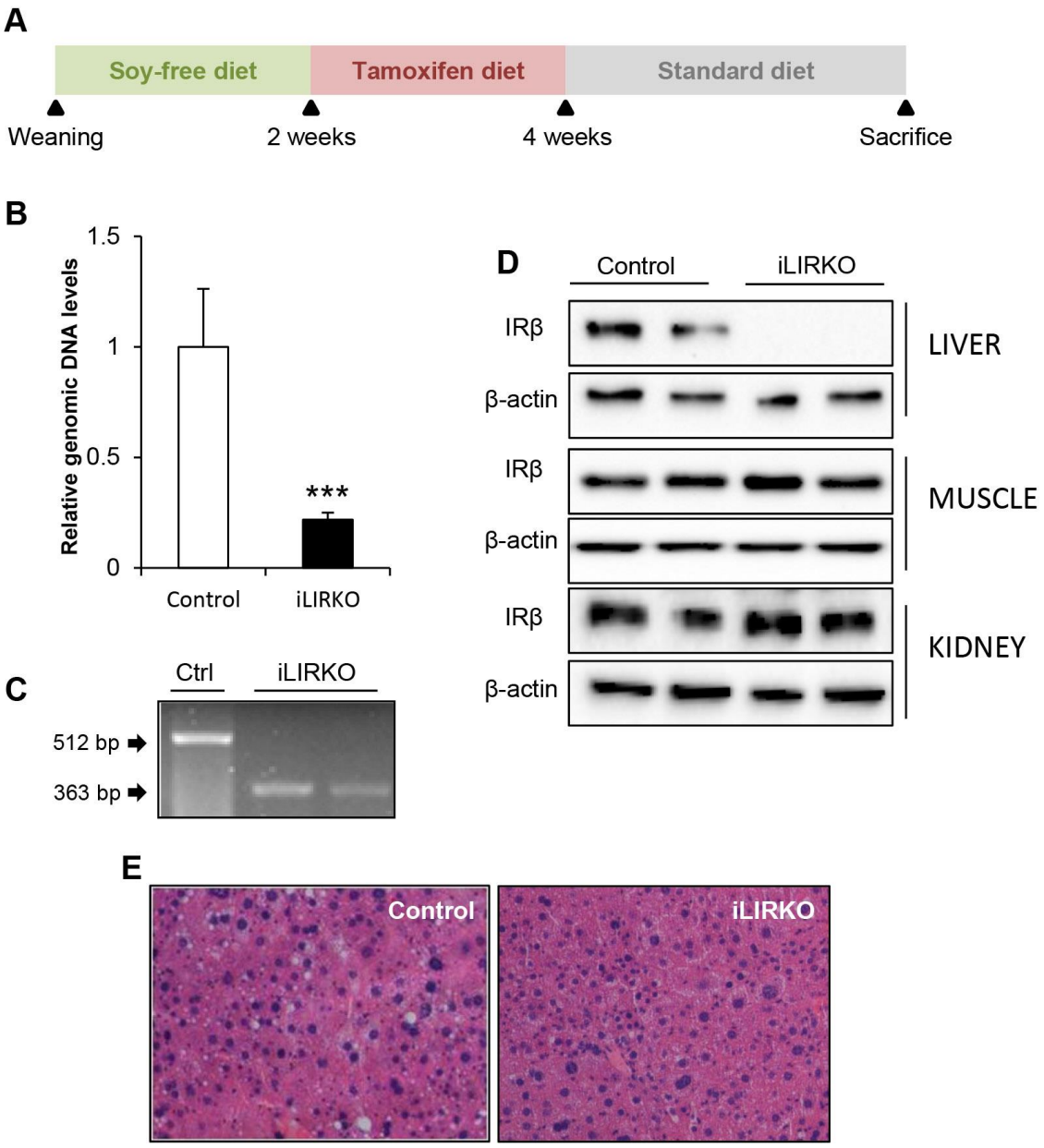

Figure 1: Generation and characterization of iLIRKO mice.

A) Schedule of diets for iLIRKO generation. B) Administration of tamoxifen diet caused *Insr* exon 4 deletion in hepatocytes. Liver isolated genomic DNA from 5-month-old mice was analyzed by qPCR. Data are means ± SEM for each experimental group (n=12). Statistical significance Control *vs* iLIRKO *(P<0.01), **(P<0.005), ***(P<0.001). C) Mouse *Insr* exon 4 deletion was

measured in livers from 5-month-old Control and iLIRKO mice by RT-PCR. D) Insulin receptor β subunit expression was analyzed by Western blot in liver, muscle and kidney homogenates obtained from 5-month-old Control and iLIRKO mice. Beta actin was used as loading control. E) Hematoxilin&Eosin staining of random liver sections from 5-month-old Control (left panel) and iLIRKO mice (right panel). Magnification 20X,

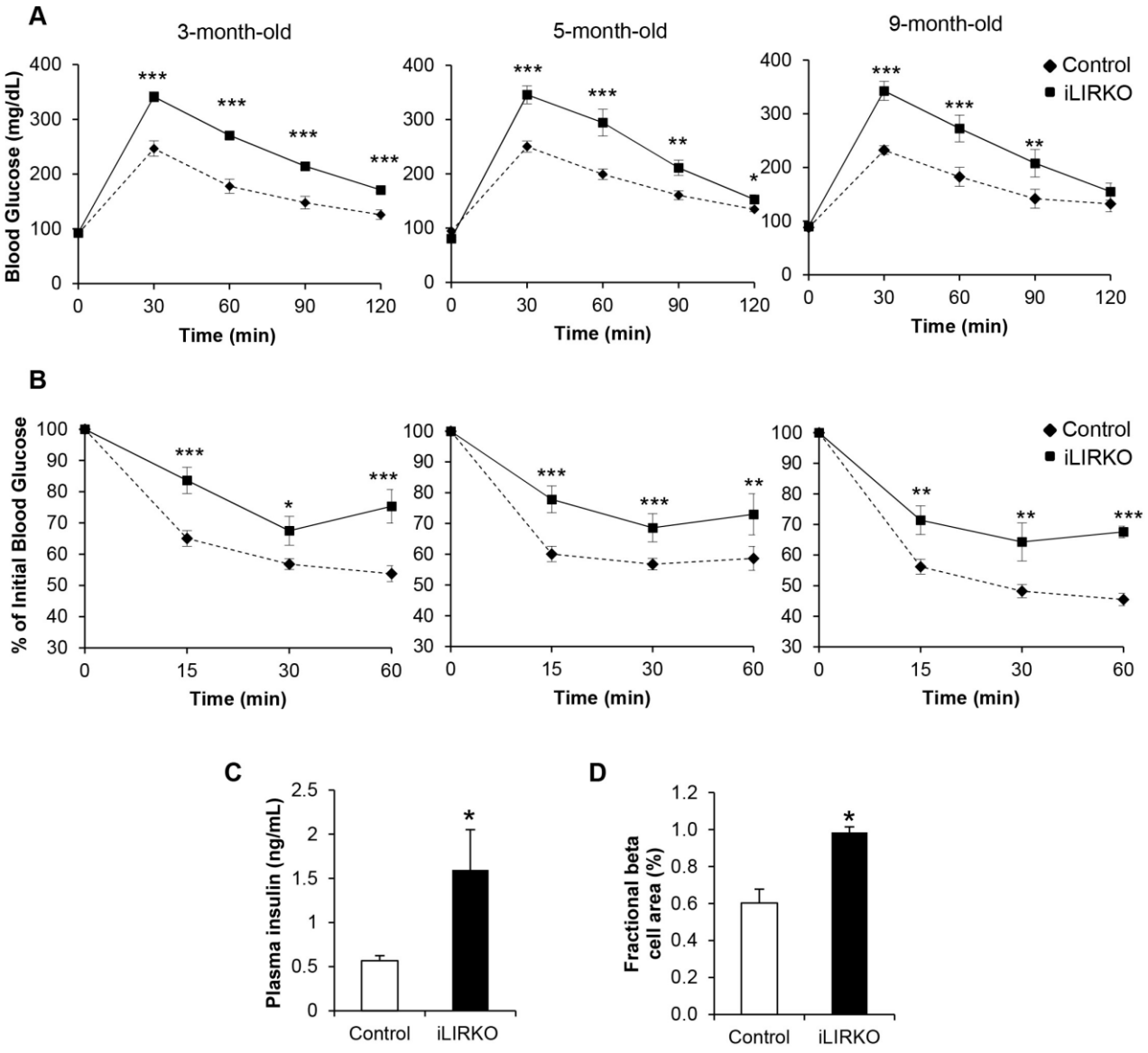

Figure 2: Metabolic effects of hepatic insulin receptor ablation.

A) Intraperitoneal glucose tolerance tests in 3, 5 and 9-month-old Control (diamonds) and iLIRKO (squares) mice (n=12 mice per group). B) Intraperitoneal insulin tolerance tests in 3, 5 and 9-month-old Control (diamonds) and iLIRKO (squares) mice (n=12 mice per group). C) Plasma insulin levels in 5-month-old Control (open bars) and iLIRKO mice (filled bars) (n=12 mice per group). D) Mean islet area in 9-month-old Control (open bars) and iLIRKO mice (filled bars) (n=5 mice per group). Data are means ± SEM for each experimental group. Statistical significance Control *vs* iLIRKO mice *(P<0.01), **(P<0.005), ***(P<0.001),

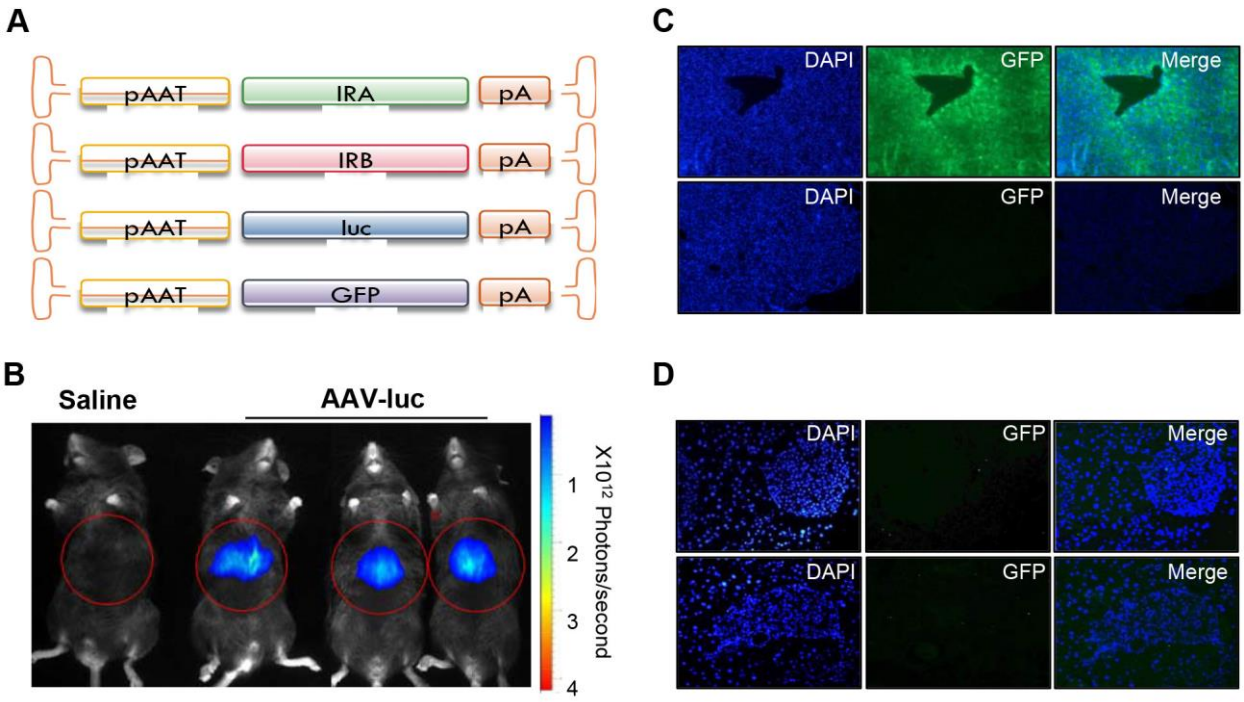

Figure 3*: In vivo* characterization of AAV-GFP- and AAV-luc-injected mice

A) Schematic diagram of Adeno-associated viral (AAV) vectors used in this study. pAAT, *human α1-antitrypsin promoter*; GFP, *green fluorescent protein* gene; IRA/B, *INSR* A or B isoform; ITR, inverted terminal repeat; *luc*, *luciferase* gene; polyA, polyadenylation signals. B) C57BL/6 mice intravenously injected with Saline solution (left) or 3×10^{10} vg/kg of AAV-luc (right) were analyzed by *in vivo* luciferase imaging 21 days after vector injection with a charge-coupled device (CCD) camera. Optical CCD images for luciferase expression of a representative animal from each group are shown. C) Representative immunofluorescences show GFP expression in the liver and (D) pancreas from AAV-GFP-injected mice 15 days after injection with 3×10^{10} vg/kg of AAV-GFP (upper panels) and negative control staining of GFP (lower panels). Magnification (C) 10X, (D) 20X.

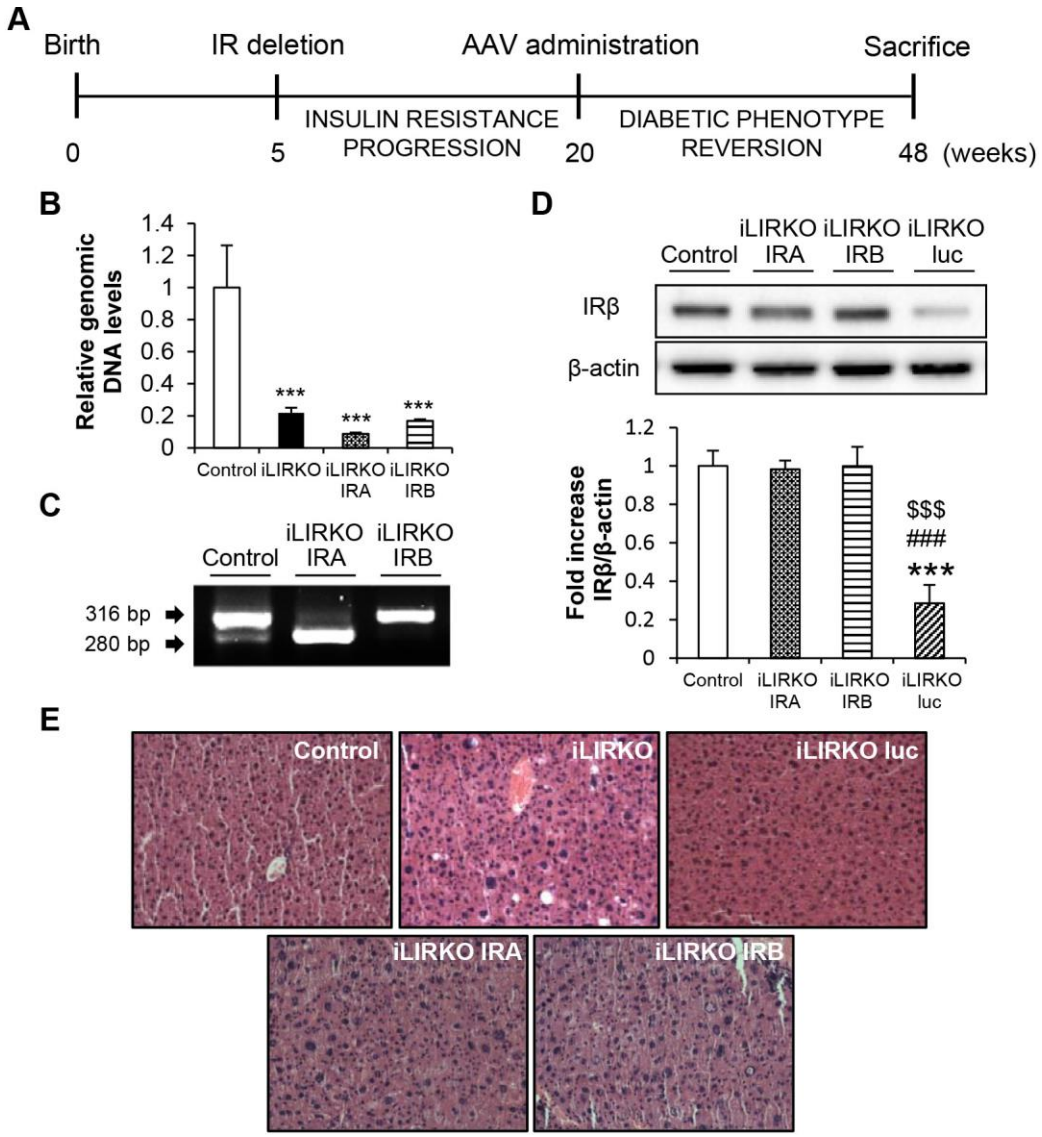

Figure 4: AAV-mediated IRA/B expression in the liver recovered initial levels of insulin receptor.

A) Schedule of AAV administration experiments. B) Mouse genomic DNA *Insr* exon 4 levels was analyzed by qPCR in 9-month-old Control and iLIRKO mice with or without AAV-IRA or AAV-IRB administration. C) Mouse *Insr* isoforms in Control and human *INSR* isoforms in iLIRKO IRA and iLIRKO IRB were analyzed by RT-PCR in livers from 9-month-old mice. D) Representative insulin receptor β subunit expression analyzed by Western blot in liver homogenates from 9-month-old Control, iLIRKO IRA, iLIRKO IRB and iLIRKO luc mice. β-actin was used as loading control. The histogram shows the band intensities quantification. Data are means ± SEM for each

experimental group, n=5. E) Representative Hematoxilin&Eosin staining of liver sections from 9-month-old Control, iLIRKO, iLIRKO luc (upper panels) and iLIRKO IRA, iLIRKO IRB (lower panels). Magnification 20X. (B,D) Statistical significance: ***(P<0.001) *vs* Control mice; ###(P<0.001) *vs* iLIRKO IRA and $$$(P<0.001) *vs* iLIRKO IRB.

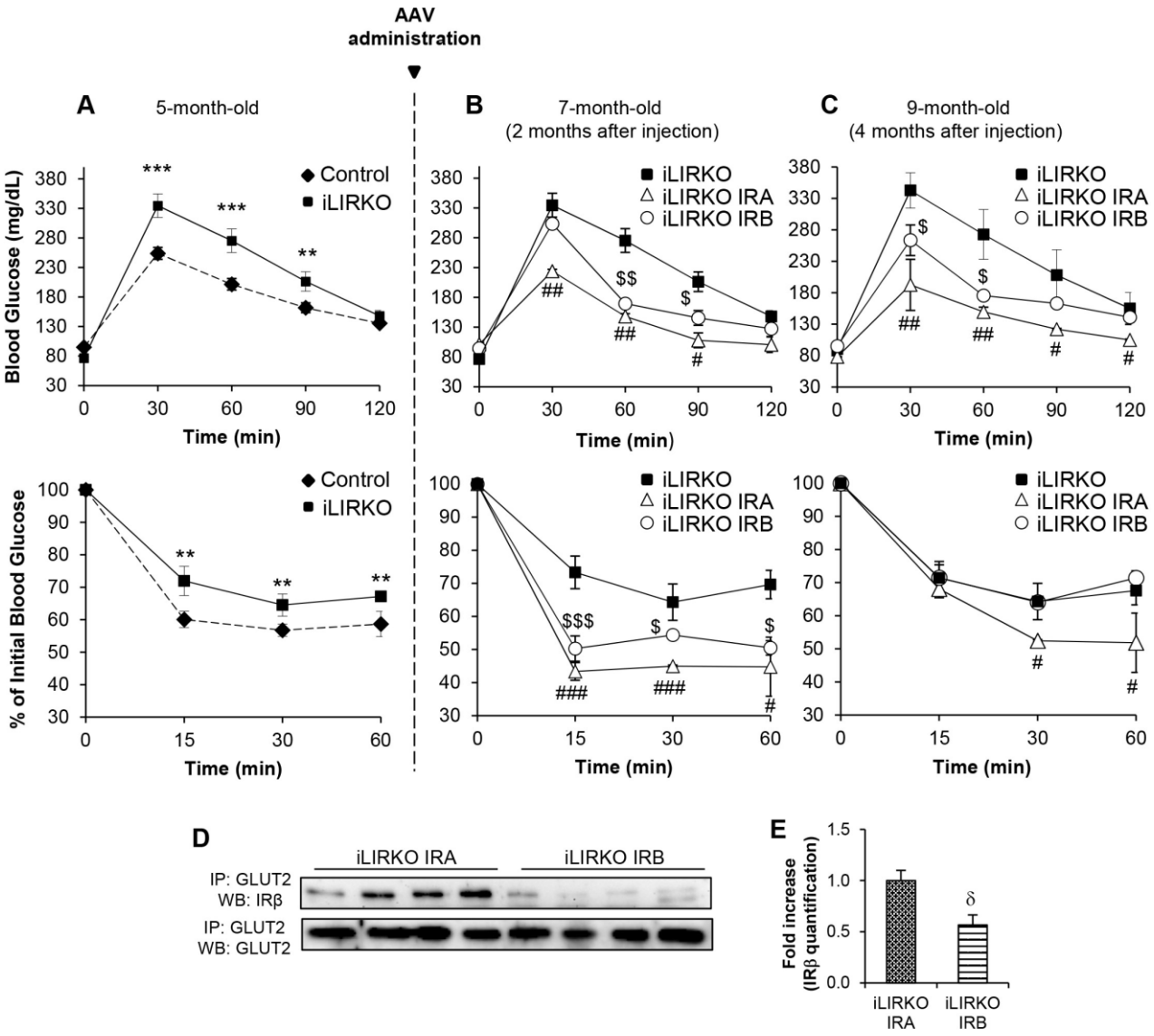

Figure 5: *In vivo* IRA expression in hepatocytes, but not IRB, reverts insulin resistance and glucose intolerance.

A) Intraperitoneal glucose (upper panel) and insulin (lower panel) tolerance tests in 5-month-old Control (diamonds) and iLIRKO mice (squares), Control mice, n=15 and iLIRKO mice n=10. (B, C) AAV-IRA or AAV-IRB were administrated in these iLIRKO mice (n=5 per isoform). GTT and ITT in 7 and 9-month-old iLIRKO (n=12), iLIRKO IRA (n=5) and iLIRKO IRB (n=5); iLIRKO IRA (white triangles), iLIRKO IRB (white circles). D) Association between GLUT2 and IR β subunit in liver homogenates from 9-month-old iLIRKO IRA (n=4) and iLIRKO IRB (n=4) mice.

Samples were subjected to immunoprecipitation (IP) and Western blot (WB). (E) Histogram of band intensities quantification. (A,B,C,E) Data are means ± SEM for each experimental group. Statistical significance Control *vs* iLIRKO **(P<0.005), ***(P<0.001); iLIRKO *vs* iLIRKO IRA #(P<0.01), ##(P<0.005), ###(P<0.001); iLIRKO *vs* iLIRKO IRB $(P<0.01), $$(P<0.005), $$$(P<0.001) and iLIRKO IRA *vs* iLIRKO IRB δ(P<0.01).

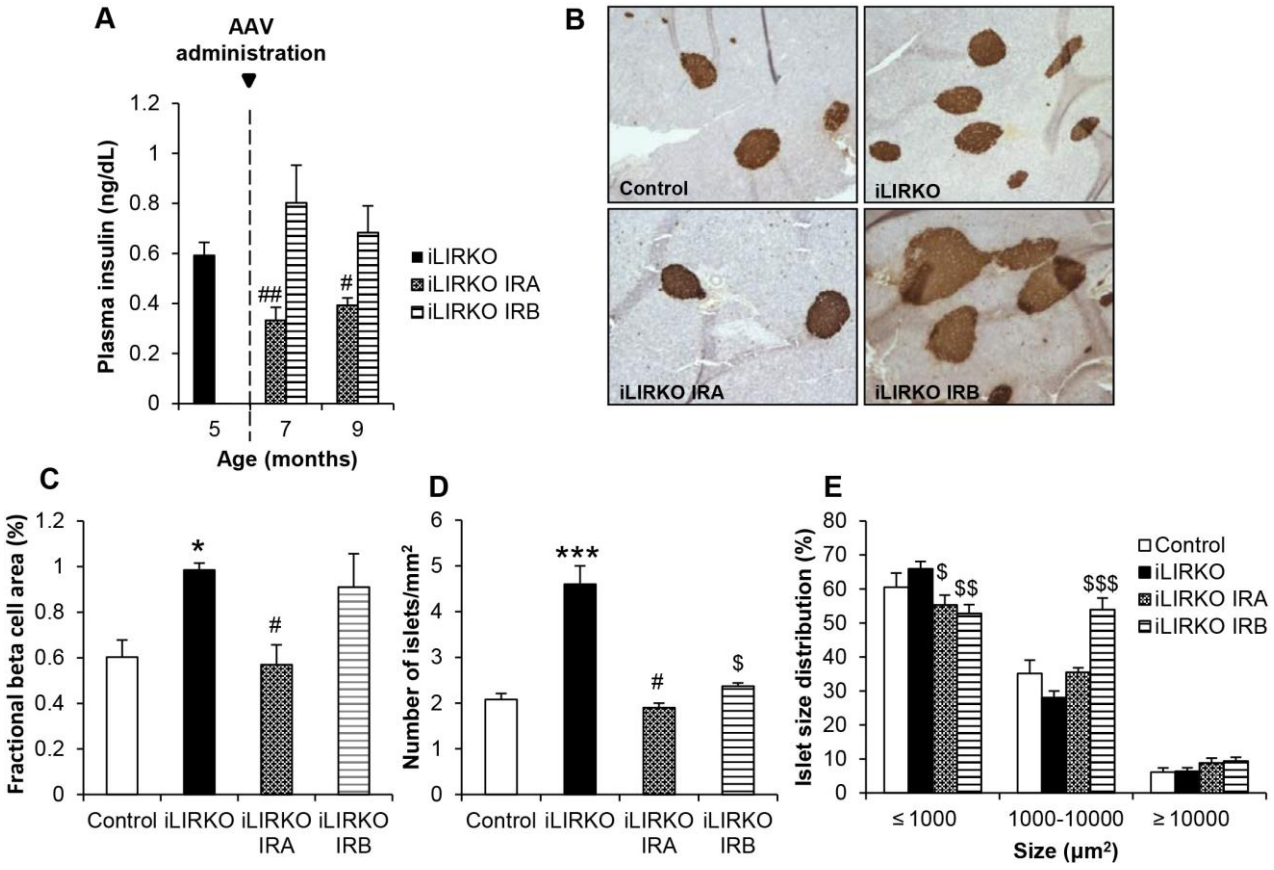

Figure 6: *In vivo* expression of IRA in hepatocytes reverts compensatory beta-cell hyperplasia.

A) Plasma insulin levels in 16 hours fasted 9-month-old mice. Data are means ± SEM for each experimental group (n=12). Statistical significance iLIRKO *vs* iLIRKO IRA #(P<0.01), ##(P<0.005). B) Representative insulin staining of pancreatic sections from 9-month-old mice of the four groups studied. Magnification 10X. C) Fractional beta-cell area (%). D) Islet density. E) Islet size distribution (%). (C-E) Data are means ± SEM for each experimental group (n=5). Control *vs* iLIRKO *(P<0.05), ***(P<0.001); iLIRKO *vs* iLIRKO IRA #(P<0.05) and iLIRKO *vs* iLIRKO IRB $(P<0.05), $$(P<0.005), $$$(P<0.001).

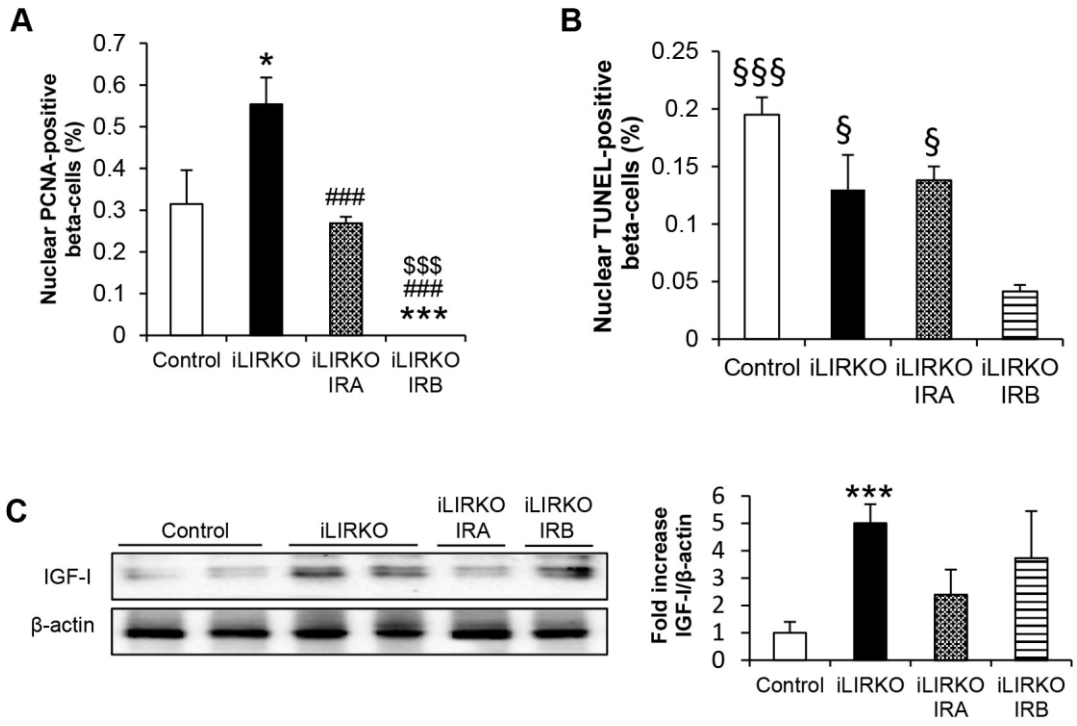

Figure 7: Hepatic IRA expression reverts beta-cell mass expansion by decreasing proliferation and hepatic IGF-I expression.

A) Quantification of nuclear PCNA and B) TUNEL positive beta cells (%). C) Representative IGF-I Western blot in liver homogenates from 9-month-old Control, iLIRKO, iLIRKO IRA and iLIRKO IRB mice. β-actin was used as loading control. The histogram shows the band intensities quantification. (A-C) Data are means ± SEM for each experimental group (n=4). *(P<0.05), ***(P<0.001) *vs* Control; ###(P<0.001) *vs* iLIRKO; $$$(P<0.001) *vs* iLIRKO IRA and §(P<0.05), §§§(P<0.001) *vs* iLIRKO IRB.